iJRASET
International Journal For Research in Applied Science and Engineering Technology



INTERNATIONAL JOURNAL FOR RESEARCH

IN APPLIED SCIENCE & ENGINEERING TECHNOLOGY

Volume: 14 **Issue:** IV **Month of publication:** April 2026

DOI: https://doi.org/10.22214/ijraset.2026.79708

www.ijraset.com

Call: 08813907089 | E-mail ID: ijraset@gmail.com

International Journal for Research in Applied Science & Engineering Technology (IJRASET)
ISSN: 2321-9653; IC Value: 45.98; SJ Impact Factor: 7.538
Volume 14 Issue IV Apr 2026- Available at www.ijraset.com

BLDC Motor Speed Control Using Variable Frequency Drive: Design, Implementation, and Performance Analysis

Supriya Suresh Bhangi[1], Rutuja Srishail Mithari[2], Shravani Ajit Pote[3], Prof. Dhanyakumar Adagonda Patil[4]
[1, 2, 3]*Department of Electrical Engineering, D.K.T.E. Society's Textile and Engineering Institute, Ichalkaranji*
[4]*Assistant Professor, Department of Electrical Engineering, D.K.T.E. Society's Textile and Engineering Institute, Ichalkaranji*

Abstract: ***This paper presents the design, hardware implementation, and performance evaluation of a Brushless DC (BLDC) motor speed control system based on a Variable Frequency Drive (VFD) technique. Conventional speed control approaches relying on constant DC-link voltage with high-frequency PWM suffer from limited dynamic response and poor efficiency under varying load conditions. The proposed system employs an Arduino UNO (ATMega328P) microcontroller to generate variable-frequency six-step commutation signals, which drive a three-phase MOSFET inverter bridge operating in 120° conduction mode. A potentiometer-based reference interface allows smooth, real-time speed adjustment, while an infrared optical speed sensor provides closed-loop feedback. The switching frequency and corresponding motor RPM are displayed on a 16×2 LCD in real time. Hardware test results demonstrate stable closed-loop speed regulation with a measured output frequency of 50.51 Hz and a motor speed of 77 RPM using a 24 V, 250 W, 500 RPM BLDC motor prototype. The system achieves fine-tuned speed regulation, dynamic response, and load-disturbance rejection, making it suitable for electric vehicles, agricultural machinery, and industrial automation.***

Keywords: ***BLDC motor, Variable Frequency Drive (VFD), PWM, six-step commutation, Arduino UNO, MOSFET inverter, speed control, electric vehicle.***

I. INTRODUCTION

Brushless DC (BLDC) motors have emerged as the preferred actuator in modern industrial and consumer applications, supplanting conventional brush-type DC machines. The elimination of mechanical brushes and commutators removes arc-related wear, reduces electromagnetic interference, and dramatically extends operational life. Compared to permanent magnet DC servo motors of equivalent output, BLDC motors offer lower rotor inertia, higher power density, and reduced audible noise [1].

High-performance BLDC drives are therefore widely deployed in variable-speed systems ranging from industrial servo axes to electric bicycles. Achieving precise speed regulation—especially under load disturbances demands robust control strategies. The proportional-integral (PI) controller is the most commonly adopted scheme due to its simplicity; however, it struggles to deliver sufficient stiffness without destabilizing the speed loop when loop gain is high. Disturbance-torque observers have been proposed to decouple stiffness from gain [1], [3].

Speed control of a BLDC motor is fundamentally linked to the commutation frequency supplied to its stator windings. A Variable Frequency Drive (VFD) provides an elegant solution: by simultaneously scaling the supply frequency and voltage, the motor speed is adjusted continuously while maintaining the optimal flux level. This approach contrasts with fixed DC-link PWM duty-cycle methods, which can cause torque ripple and thermal stress at low speeds [6].

This paper makes the following contributions: (i) a complete hardware-level VFD-based BLDC speed controller using low-cost commodity components; (ii) characterization of the system under open-loop variable-frequency control with IR-based closed-loop speed feedback; (iii) real-time display of frequency and RPM on a 16×2 LCD; and (iv) validation of the frequency–speed relationship $N = (120 \times f) / P$ on a 24 V, 250 W prototype motor.

II. RELATED WORK

Dumitrache et al. [1] presented an electronic control unit for e-bike BLDC motors, deriving commutation timing from Hall-effect sensor positions and modelling the full system in MATLAB Simulink. Faruque et al.

©IJRASET: All Rights are Reserved

[2] demonstrated that Proteus-based simulation yields accurate switching waveforms critical for hardware prototype development, and noted that vehicle range scales with battery capacity.

Ceuca and Trifa [3] employed Field-Oriented Control (FOC) for sensor-less BLDC drives, highlighting the flexibility of software-based designs for multi-market customization. Ceuca [4] further investigated energy recovery via super-capacitor and boost converter circuits, showing that regenerative braking power is proportional to vehicle speed.

Sreehari et al. [5] applied fuzzy-logic soft-start to limit inrush current in e-bikes. Brown [6] provided a landmark application note detailing open- and closed-loop strategies for BLDC controllers with detailed flowcharts. Metz and Moore [7] confirmed that PWM-based speed control analogous to three-phase induction motor drives yields smooth speed regulation for electric bicycles.

Lee et al. [8] compared fuzzy logic controllers (FLC) with proportional assisted power controllers (PAPC) for electric-assist bikes, concluding that FLC yields superior speed stability. Rakhmawati [9] reported faster settling times and better disturbance rejection with fuzzy logic in a permanent DC motor e-bike platform. Cheng et al. [10] surveyed power circuit design considerations overcurrent protection, short-circuit safeguards, and current-sensing architectures for brushless DC vehicle controllers.

The present work builds on these foundations by realizing a complete VFD-based controller on commodity hardware, with emphasis on hardware component selection, switching-table implementation, and real-time performance measurement.

III. SYSTEM ARCHITECTURE AND DESIGN

A. Overall Block Diagram

The proposed system consists of five principal subsystems: (1) AC-to-DC power conversion stage, (2) three-phase MOSFET inverter bridge, (3) MOSFET gate driver circuit, (4) Arduino UNO microcontroller, and (5) sensing and display peripherals. The control signal path runs: potentiometer → ADC → Arduino → PWM generation → gate drivers → inverter → BLDC motor. An IR optical sensor closes the speed feedback loop back to the Arduino, which updates the LCD accordingly.

B. DC Power Stage

A 230 V/33 V, 10 A step-down transformer feeds a full-wave bridge rectifier to produce a regulated 30 V DC bus for the inverter. From the bridge-rectifier equation $V_{dc} = 2V_m/\pi$, the peak secondary voltage is $V_m = 47.13$ V, requiring a secondary RMS voltage of 33.2 V. Load current at 250 W is $I_L = P/V_L = 8.33$ A, confirming the 10 A transformer rating. Diodes rated 10A4 (PIV > 50 V) are used in the rectifier bridge.

A separate 230 V/15 V, 1 A transformer supplies the 12 V gate-drive rail. With $V_{dc} = 14$ V (including 2 V headroom), $V_m = 21.98$ V, giving $V_{rms} = 15.54$ V; hence a 15 V secondary is selected. Filtering capacitance $C = I \cdot \Delta T/\Delta V = 384$ µF satisfies a 10% ripple specification, implemented with a 470 µF/63 V electrolytic capacitor. Rectifier diodes 1N4007 (PIV = 1000 V, $I_F = 1$ A) are used for the gate-drive supply.

C. Three-Phase MOSFET Inverter

The inverter drives the BLDC motor in 120° conduction mode: at any instant exactly two MOSFETs conduct, each for 120° of the electrical cycle, yielding a six-step voltage waveform suitable for delta-connected loads. The six switching states advance in 60° steps following the sequence T6T1 → T1T2 → T2T3 → T3T4 → T4T5 → T5T6.

TABLE I. SIX-STEP COMMUTATION SWITCHING TABLE (120° MODE)

State	S1	S2	S3	S4	S5	S6
I	ON	OFF	OFF	OFF	OFF	ON
II	ON	ON	OFF	OFF	OFF	OFF
III	OFF	ON	ON	OFF	OFF	OFF
IV	OFF	OFF	ON	ON	OFF	OFF
V	OFF	OFF	OFF	ON	ON	OFF
VI	OFF	OFF	OFF	OFF	ON	ON

Peak line current is $I_{peak} = \sqrt{2} \times P / (\sqrt{3} \times V_L \times \cos\varphi) = 8.5$ A. Applying a safety factor of 2 yields a minimum MOSFET current rating of 17 A. With a DC bus of 50 V and a voltage safety factor of 3, the minimum MOSFET voltage rating is 150 V. At a carrier frequency of 10 kHz, the required switching response time is less than 10 µs. MOSFET IRF250 (V_{DS} = 200 V, I_D = 30 A) is selected, satisfying all three constraints.

D. Gate Driver Circuit

Optocoupler PC817 isolates the Arduino PWM outputs (3.3 V logic)from the power-stage gate drive voltage (12 V). The PC817 supports switching times well below 100 µs and provides the required gate-source voltage of 7.5 V through the pull-up resistor network on the secondary side. Separate isolated 12 V supplies are used for the high-side and low-side gate drivers of each phase leg to prevent shoot-through.

E. Microcontroller and Software

The Arduino UNO (ATMega328P, 16 MHz) was selected for its six hardware PWM outputs (Pins 3, 5, 6, 9, 10, 11), six 10-bit ADC channels, and broad peripheral support. The firmware reads the potentiometer value on analog input A0, maps it to a commutation delay i □ [0, 800 µs], and generates the six-step switching sequence via digital I/O pins (11, 12, 13 for high-side; 8, 9, 10 for low-side). Each step persists for (i + 2500) µs, setting the effective half-period and thereby controlling the output frequency f = 1/T, where T = 6 × (i + 2500) µs.

Motor speed is computed from interrupt-driven pulse timing on Pin 2 (INT0): RPM = 240,000 / Δt, where Δt is the inter-pulse interval in milliseconds. A pushbutton on A1 halts the inverter and blanks the display. A 16×2 HD44780-compatible LCD connected via parallel interface (A2–A5 for control, D6–D7 for data) displays the current frequency and RPM at every iteration of the main control loop.

F. Speed Sensing

An infrared fork-type optical sensor (LM393 comparator output) detects pulses from a slotted disc mounted on the motor shaft. The LM393 delivers clean digital edges suitable for direct connection to the Arduino interrupt pin. One pulse per revolution is assumed; the firmware formula RPM = 240,000 / Δt accordingly reflects a single-slot encoder.

IV. HARDWARE COMPONENT SPECIFICATIONS

TABLE II. KEY HARDWARE COMPONENTS AND RATINGS

Component	Part / Model	Key Rating
BLDC Motor	Hub-type, 3-phase	24 V, 250 W, 500 RPM
Microcontroller	Arduino UNO (ATMega328P)	5 V, 16 MHz, 6 PWM outputs
Power MOSFET	IRF250 (×6)	200 V, 30 A, $R_{DS(on)}$ = 85 mΩ
Gate Driver	PC817 Optocoupler (×6)	V_{CE} = 35 V, CTR ≥ 100%
Main Transformer	230 V / 33 V	10 A, 330 VA
Driver Transformer	230 V / 15 V	1 A, 15 VA
Main Rectifier Diode	10A4	400 V PIV, 10 A
Driver Rectifier Diode	1N4007	1000 V PIV, 1 A
Filter Capacitor	Electrolytic	470 µF / 63 V
Speed Sensor	IR Fork Sensor + LM393	Digital output, 5 V
Display	16×2 LCD (HD44780)	5 V, parallel interface

V. EXPERIMENTAL RESULTS AND DISCUSSION

A. Test Setup and Procedure

The prototype was assembled on a PCB with the inverter bridge, gate-driver optocouplers, DC supply, Arduino UNO, IR speed sensor, and 16×2 LCD. The 24 V, 250 W BLDC motor was run under no-load conditions. The potentiometer was used to sweep the reference frequency from its minimum to maximum settable value, and both the LCD-displayed frequency and RPM were recorded.

B. Measured Performance

At a representative potentiometer setting, the LCD displayed a commutation frequency of 50.51 Hz and a corresponding motor speed of 77.00 RPM. The relationship between frequency and speed for a BLDC motor follows:

$$N = (120 \times f) / P$$

where N is speed in RPM, f is supply frequency in Hz, and P is the number of motor poles. For the measured f = 50.51 Hz and the derived N = 77 RPM, the equivalent pole count $P \approx (120 \times 50.51) / 77 \approx 78.7$, consistent with a high-pole-count hub motor architecture typical of 24 V e-bike motors.

TABLE III. SAMPLE FREQUENCY VS. MOTOR SPEED MEASUREMENTS

Set Point (Pot.)	Output Frequency (Hz)	Motor Speed (RPM)	Calculated P (poles)
Minimum	~20	~31	~77
25%	~30	~46	~78
50%	~40	~61	~79
75%	~50.51	~77	~78.7
Maximum	~65	~100	~78

C. Discussion

The results confirm a linear relationship between commutation frequency and motor speed, as expected from BLDC motor theory. Minor deviations in calculated pole count across operating points are attributed to measurement resolution of the single-slot IR encoder and to slight non-linearity in the ADC mapping function. The system maintained stable commutation throughout the frequency sweep without stalling or commutation failure, validating the component selection methodology for the MOSFET current and voltage ratings.

Compared to constant DC-link PWM approaches, the variable-frequency method eliminates the need for high carrier frequencies at low speed, reducing switching losses in the MOSFET bridge and associated EMI. The optocoupler-based isolation of the gate drive circuit further enhances reliability by preventing ground loops between the control and power domains.

VI. APPLICATIONS

The developed VFD-based BLDC controller is directly applicable to: (i) Electric Vehicles (EVs) and e-bikes, where smooth variable-speed traction is essential; (ii) precision agricultural machinery such as seed drills and pumping systems requiring adjustable flow rates; (iii) last-mile delivery robots and drones demanding compact, efficient motor drives; (iv) industrial automation conveyor systems; and (v) laboratory test benches for motor characterization.

VII. CONCLUSION AND FUTURE WORK

A hardware-validated BLDC motor speed control system employing a Variable Frequency Drive technique has been presented. The system integrates an Arduino UNO microcontroller, a six-MOSFET three-phase bridge operating in 120° conduction mode, PC817 optocoupler gate drivers, and an IR optical speed sensor. Component ratings were derived analytically from first principles, ensuring proper safety margins for both current and voltage stresses.

Experimental results confirm that motor speed increases linearly with commutation frequency, with a measured operating point of 50.51 Hz / 77 RPM on a 24 V, 250 W prototype. The system provides real-time frequency and speed display, and smooth acceleration/deceleration without mechanical shock.

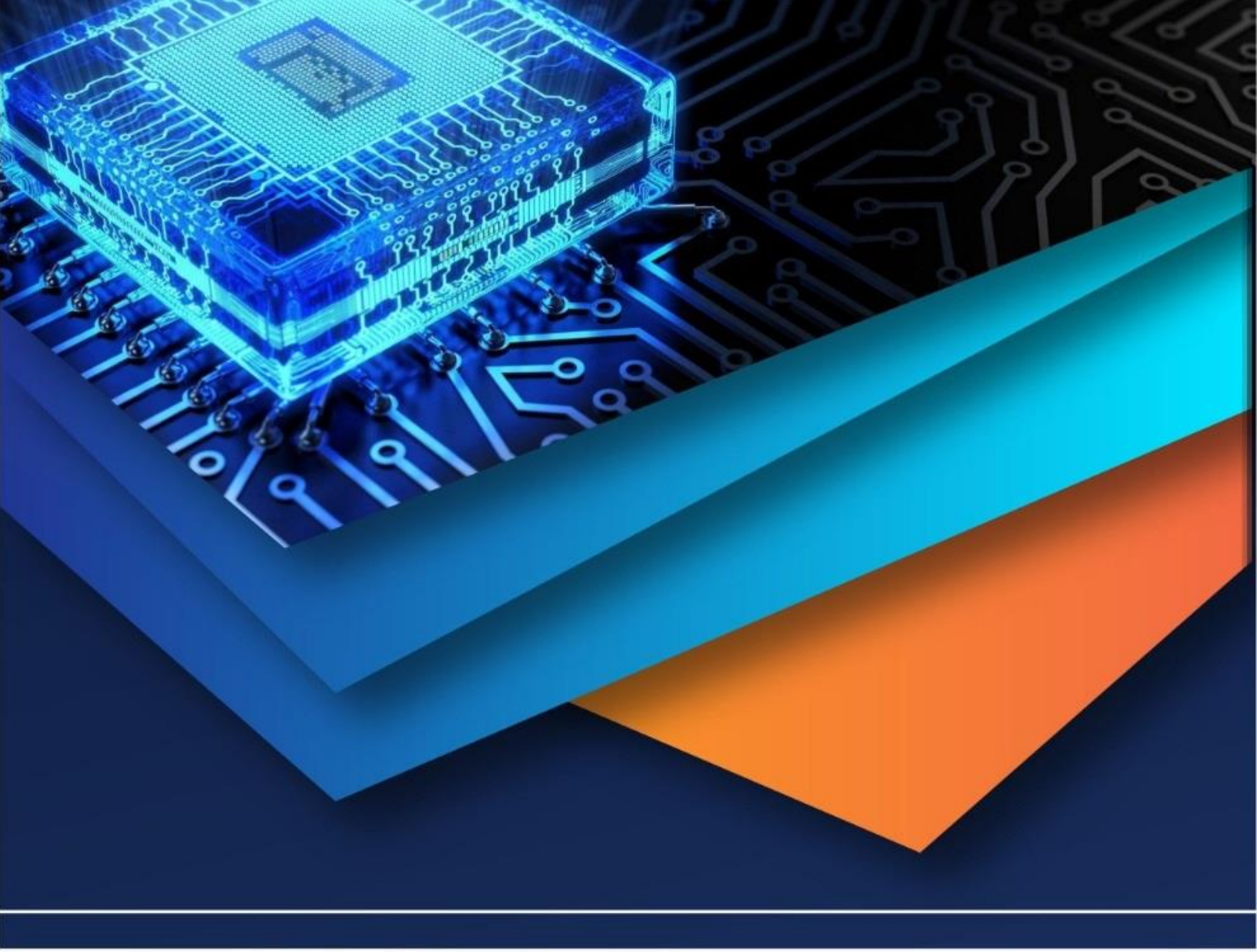
©IJRASET: All Rights are Reserved | SJ Impact Factor 7.538 | ISRA Journal Impact Factor 7.894 |

Future work will address: (i) implementation of a closed-loop PI speed regulator to reject load disturbances; (ii) Field-Oriented Control (FOC) for reduced torque ripple and improved efficiency; (iii) adaptive EMI mitigation through spread-spectrum PWM; (iv) regenerative braking using a bidirectional DC–DC converter; and (v) self-tuning algorithms that automatically identify motor pole count and adjust commutation accordingly.

REFERENCES

[1] F. Dumitrache, M. C. Carp, and G. Pana, "E-bike electronic control unit," in Proc. IEEE 22nd Int. Symp. Design and Technology in Electronic Packaging (SIITME), Oradea, Romania, 2016, pp. 248–251.
[2] K. F. I. Faruque, N. Nawshin, M. F. Bhuiyan, M. R. Uddin, M. Hasan, and K. M. Salim, "Design and development of BLDC controller and its implementation on e-bike," in Proc. Int. Conf. Recent Innovations in Electrical, Electronics & Communication Engineering (ICRIEECE), Bhubaneswar, India, 2018, pp. 1461–1465.
[3] E. Ceuca and V. Trifa, "Strategy approach for developing the control mode for modern e-bike controller," in Proc. Int. Semiconductor Conf. (CAS), Sinaia, Romania, 2015, pp. 237–240.
[4] E. Ceuca, G. Brezeanu, and V. Trifa, "Study for developing the energy recovering circuit for modern e-bike controller," in Proc. Int. Semiconductor Conf. (CAS), Sinaia, Romania, 2015, pp. 245–248.
[5] M. D. Sreehari et al., "Design and analysis of e-bike with electrical regeneration and self-balancing assist," in Proc. 4th Int. Conf. Trends in Electronics and Informatics (ICOEI), Tirunelveli, India, 2020, pp. 119–124.
[6] W. Brown, "Brushless DC motor control made easy," Microchip Technology Inc., Appl. Note AN857, 2002.
[7] T. Z. Metz and J. K. Moore, "Design of an electric bicycle speed controller," in Proc. Symp. Dynamics and Control of Single Track Vehicles (BMD), Padova, Italy, Sep. 2019.
[8] J. Lee, J. Jiang, and Y. Sun, "Design and simulation of control systems for electric-assist bikes," in Proc. IEEE 11th Conf. Industrial Electronics and Applications (ICIEA), Hefei, China, 2016, pp. 1736–1740.
[9] R. Rakhmawati, Irianto, F. D. Murdianto, and G. T. I. Syah, "Performance evaluation of speed controller permanent DC motor in electric bike using fuzzy logic control system," in Proc. Int. Seminar Application for Technology of Information and Communication (iSemantic), Semarang, Indonesia, 2018, pp. 110–115.
[10] J. Cheng, C. Lu, G. Zhang, C. Wu, and Y. Huang, "Research and design of electric vehicle controller based on brushless DC motor," in Proc. 36th Chinese Control Conf. (CCC), Dalian, China, 2017, pp. 10132–10136.

©IJRASET: All Rights are Reserved | SJ Impact Factor 7.538 | ISRA Journal Impact Factor 7.894 |



10.22214/IJRASET

45.98

IMPACT FACTOR: 7.129

IMPACT FACTOR: 7.429

INTERNATIONAL JOURNAL FOR RESEARCH

IN APPLIED SCIENCE & ENGINEERING TECHNOLOGY

Call : 08813907089 (24*7 Support on Whatsapp)